CrossMark

RESEARCH PAPER

Energy-Based Estimation of Soil Liquefaction Potential Using GMDH Algorithm

Hamed Javdanian[1] · Ali Heidari[1] · Reza Kamgar[1]

Abstract Reliable determination of seismic liquefaction potential of soil is an important obligation in earthquake engineering. In this study, neuro-fuzzy group method of data handling (NF-GMDH) was employed for prediction of strain energy required to induce liquefaction. The NF-GMDH-based model was developed using particle swarm optimization. A wide-ranging database of soil element tests was used to develop an advanced model, capable of predicting soil liquefaction resistance accurately. Input variables of the model were chosen based on the previous studies on the liquefaction potential assessment. Results of geotechnical centrifuge tests were also involved during the training process for adequate generalization of the proposed model for future predictions. A parametric analysis was then performed to evaluate sensitivity of the proposed model to variations of the influencing parameters. A comparison between performance of the developed model and previously recommended relationships was done. The results clearly demonstrate that the proposed model, which was derived based on laboratory results, can be successfully utilized for strain energy-based estimation of liquefaction potential.

Keywords Liquefaction · Sand · Strain energy · NF-GMDH · PSO

✉ Hamed Javdanian
javdanian@eng.sku.ac.ir

[1] Department of Civil Engineering, Shahrekord University, Shahrekord, Iran

1 Introduction

Liquefaction is the phenomena when there is loss of strength in saturated and cohesionless soils because of increased pore water pressures and hence reduced effective stresses due to dynamic loading. After the disastrous damage observed during the Niigata and Alaska 1964 earthquakes, the liquefaction phenomenon has become the scope of many studies in the field of geotechnical earthquake engineering (e.g., Lee and Fitton 1969; Seed and Idriss 1971; Seed et al. 1975; Dabiri et al. 2011). Several methods are developed to assess the liquefaction potential in the field. The available methods for evaluation of liquefaction are classified into three main groups (Green 2001; Alavi and Gandomi 2012): stress-based methods, strain-based methods and energy-based methods.

The most widely used method for evaluating liquefaction is the stress-based approach. This method was proposed by Seed and Idriss (1971) and Whitman (1971). Stress-based method is mainly empirical and is based on laboratory and field data. In this approach to correlate real earthquake motion to laboratory harmonic loading condition, the equivalent shear stress level, the number of cycles and the equivalent earthquake duration should be defined such that differences are always available between the results of researches (Ishihara and Yasuda 1975; Seed et al. 1975; National Research Council 1985; NCEER 1997). Although this approach has been continually modified as a result of newer studies and the increase in the number of liquefaction case histories (e.g., NCEER 1997; Youd et al. 2001), this deficiency still persists. Dobry et al. (1982) proposed the strain-based method as an alternative to the empirical stress-based procedure. This method was derived from the mechanics of two interacting idealized sand grains and then generalized for natural soil deposits (Green 2001;

Springer

Baziar and Jafarian 2007). The strain-based method has been less common than the stress-based method because of the fact that the strain approach only predicts the initiation of pore pressure buildup, which is required for liquefaction occurrence, but does not imply that liquefaction will happen.

Energy-based assessment of liquefaction potential considers effects of strain and stress concurrently, unlike the stress- or strain-based procedures (Liang 1995; Baziar et al. 2011). In the energy-based method, the amount of strain energy required to trigger liquefaction in sandy soils is obtained from laboratory testing or field data. Figure 1 represents a schematic of shear stress–strain curve (hysteresis loop) from a cyclic triaxial test. The area inside the hysteresis loop represents the dissipated energy per unit volume of the soil mass. The summation of energy is computed until the onset of liquefaction phenomena. For prediction of liquefaction triggering, this strain energy is compared with the strain energy divulged by dynamic loading such as earthquake to the sand layer during the seismic design event (Jafarian et al. 2011).

The progress of advanced computational methods for problems analysis necessitates the accurate determination of soil liquefaction potential. In recent years, new aspects of modeling, optimization and problem solving have evolved in light of the pervasive development in computational software and hardware. These aspects of software engineering are referred to as soft computing-based methods such as artificial intelligence which is a powerful tool for multivariate and nonlinear modeling. In case of complicated problems, experimentalists prefer these trial approaches rather than analytical optimization. Numerous researchers applied artificial intelligence models for or prediction in the various topics of geotechnical and structural engineering such as stress–strain modeling of soil
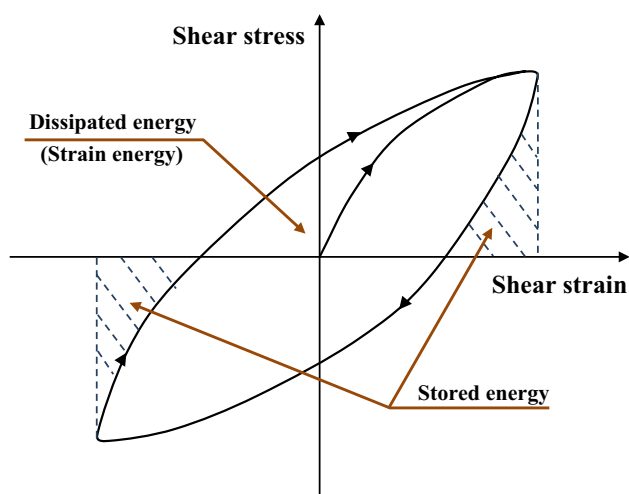

Fig. 1 Hysteretic stress–strain curve for cyclic loading

(Penumadu and Zhao 1999), slope stability (McCombie and Wilkinson 2002), landslide (Oh and Pradhan 2011), settlement of shallow foundations (Shahin et al. 2002), bearing capacity of reinforced footings (Javdanian et al. 2012), groundwater (Tabesh and Dini 2009; Rakhshandehroo and Ghadampour 2011), liquefaction (Baykasoglu et al. 2009), retaining wall (Heidari 2011), dynamic soil properties (Jafarian et al. 2014; Javdanian et al. 2015), predicting scour depth (Najafzadeh and Azamathulla 2013a, b; Najafzadeh et al. 2014) and dynamic analysis of structures (Salajegheh and Heidari 2004; Heidari and Salajegheh 2006; Heidari 2010).

In the past years, the GMDH networks provided successful evaluations in various fields of geotechnical engineering sciences such as prediction of the scour depth around hydraulic structures (Najafzadeh et al. 2013a, b; Najafzadeh et al. 2014a, b) and estimation of the S_u-N_{SPT} correlation (Kalantary et al. 2009). Application of the GMDH networks yielded relatively precise estimations than those obtained using empirical equations-based regressive models. The main concern of the GMDH network is to present analytical solutions for various problems within a feed-forward network in the form of quadratic polynomial whose weighting coefficients are obtained using regression method (Najafzadeh et al. 2013a, b; Kalantary et al. 2009).

In recent decades, the structure of the GMDH network has been improved using multistage fuzzy decision rule as neuro-fuzzy GMDH to obtain physical insights of problems with high degree of complexity. The NF-GMDH networks have been successfully applied to the different problems such as grinding characteristics and forecasting the unreliable mobile communication (Nagasaka et al. 1995; Hwang 2006). The neuro-fuzzy GMDH has higher flexibility and lower complexity compared to the GMDH network. The other advantages of the NF-GMDH models were presented in the literature (Najafzadeh and Azamathulla 2013a, b; Najafzadeh and Lim 2014; Najafzadeh 2014).

In this paper, a new approach is introduced based on NF-GMDH model for assessment of the soil liquefaction potential. The GMDH-based model is trained and tested separately using two different datasets of laboratory tests results. Also, the particle swarm optimization (PSO) algorithm is applied in topology design of the NF-GMDH model for prediction of the liquefaction triggering. The performance of the proposed model is also evaluated through centrifuge validation set. A parametric analysis was carried out to evaluate the sensitivity of the proposed model to the variation of the influencing parameters. The results of the developed model are compared with those obtained from the previous empirical and statistical relationships. It is shown that the NF-GMDH models are able to learn with a high accuracy for the complex correlation

between liquefaction potential and its influencing factors. It is clear that a precise correlation is easier to use in the routine geotechnical projects compared with the field measurement techniques.

2 Methodology

2.1 Framework of Neuro-Fuzzy GMDH

The GMDH network is a learning machine based on the principle of heuristic self-organizing, designed by Ivakhnenko (1971). Also, it is a series of operations of seeding, rearing, crossbreeding, selection and rejection of seeds that correspond to the determination of the input variables, structure and parameters of model, and selection of model by principle of termination (Madala and Ivakhnenko 1994). The other descriptions of GMDH network were presented in the literature (Onwubolu 2008).

In this paper, a neuro-fuzzy GMDH model-based PSO algorithm has been proposed for liquefaction potential prediction. The structure of neuro-fuzzy GMDH is constructed automatically using heuristic self-organized algorithm (Hwang 2006). The neuro-fuzzy GMDH network is a very flexible algorithm, and it can be hybridized easily by other iterative and evolutionary algorithms. Furthermore, a simplified fuzzy reasoning rule is utilized to improve the GMDH network as follows (Ohtani et al. 1998):

$$F_{kj}(x_j) = \exp\left(-\left(x_j - a_{kj}\right)^2 / b_{kj}\right) \tag{1}$$

If x_1 is F_{k1} and x_2 is F_{k2}, then output y is w_k. Gaussian membership function is used in terms of F_{kj} which is related to the kth fuzzy rules in the domain of the jth input values x_j. Parameters a_{kj} and b_{kj} are constant values for each rule. Also, y parameter is defined as output that has been expressed as follows:

$$y = \sum_{k=1}^{K} u_k w_k \tag{2}$$

$$u_k = \prod_{j} F_{kj}(x_j) \tag{3}$$

where w_k is real value for kth fuzzy rules (Hwang 2006; Ohtani et al. 1998).

NF-GMDH model is one of the adaptive learning networks that have hierarchical structure. In this model, each neuron has two input variables and one output. General configuration of NF-GMDH is indicated in Fig. 2. As depicted in Fig. 2, output of each neuron in a layer is considered as the input variable in the next layer. The final output is calculated using average of the outputs from the last layer. As shown in Fig. 2, the inputs from the mth model and pth layer are the output variables of the (m-1)th
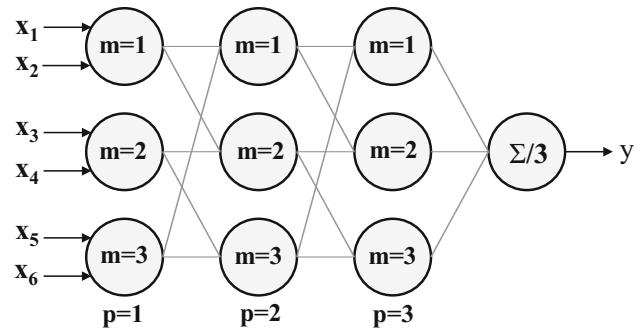

Fig. 2 A feed-forward network for the NF-GMDH model

and mth model in the (p-1)th layer. The mathematical function for calculating the y^{pm} is:

$$y^{pm} = f\left(y^{p-1,m-1}, y^{p-1,m}\right) = \sum_{k=1}^{K} \mu_k^{pm} . w_k^{pm} \tag{4}$$

$$\mu_k^{pm} = exp\left\{ -\frac{\left(y^{p-1,m-1} - a_{k,1}^{pm}\right)^2}{b_{k,1}^{pm}} - \frac{\left(y^{p-1,m} - a_{k,2}^{pm}\right)^2}{b_{k,2}^{pm}} \right\} \tag{5}$$

where μ_k^{pm} and w_k^{pm} are the kth Gaussian function and its corresponding weight parameter, respectively, that are related to the mth model in the pth layer.

In addition, a_k^{pm} and b_k^{pm} are the Gaussian parameters that are utilized for the ith input variable from the mth model and pth layer. Also, final output is expressed using the following function:

$$y = \frac{1}{M} \sum_{m=1}^{M} y^{pm} \tag{6}$$

The learning process of feed-forward neuro-fuzzy GMDH is known as an iterative method to solve the complicated systems. In each iteration, error parameter for network can be obtained as follows:

$$E = \frac{1}{2}(y^* - y)^2 \tag{7}$$

where y^* is the predicted value.

2.2 Development of NF-GMDH Using PSO Algorithm

In this research, the NF-GMDH model is developed using particle swarm optimization (PSO) algorithm. The basic structure of the NF-GMDH network consists of partial descriptions. As mentioned in the previous section, grouped parameters in the form of Gaussian variables and weighting coefficients related to the fuzzy rule are unknown in each partial description (PD). The PSO algorithm is applied to optimize grouped-unknown parameters in PDs.

The particle swarm optimization (PSO) was inspired by the social behavior of animals such as fish schooling, insects swarming and birds flocking. PSO was introduced by Kennedy and Eberhart (1995) to simulate the graceful motion of bird swarms as a part of a socio-cognitive study. It involves a number of particles that are initialized randomly in the search space of an objective function. These particles are referred to as swarm. Each particle of the swarm represents a potential solution of the optimization problem. The ith particle in tth iteration is associated with a position vector, X_i^t, and a velocity vector, V_i^t, that are shown as follows:

$$X_i^t = \left\{ x_{i1}^t, x_{i2}^t, \ldots, x_{iD}^t \right\} \tag{8}$$

$$V_i^t = \left\{ v_{i1}^t, v_{i2}^t, \ldots, v_{iD}^t \right\} \tag{9}$$

where D is dimension of the solution space.

The particle flies through the solution space and its position is updated based on its velocity, the best position particle (pbest) and the global best position (gbest) that swarms have visited since the first iterations are:

$$V_i^{t+1} = \omega^t V_i^t + c_1 r_1 \left(\text{pbest}_i^t - X_i^t \right) + c_2 r_2 \left(\text{gbest}_i^t - X_i^t \right) \tag{10}$$

$$X_i^{t+1} = X_i^t + V_i^{t+1} \tag{11}$$

where r_1 and r_2 are two uniform random sequences generated from interval [0, 1]; c_1 and c_2 are the cognitive and social scaling parameters, respectively; and ω^t is the inertia weight that controls the effect of the previous velocity.

Shi and Eberhart (1998) proposed that the cognitive and social scaling parameters c_1 and c_2 should be selected as $c_1 = c_2 = 2$ to allow the product $c_1 r_1$ or $c_2 r_2$ to have a mean of 1. The performance of PSO is very sensitive to the inertia weight (ω) parameter which may decrease with the number of iterations as follows (Shi and Eberhart 1998):

$$\omega = \omega_{\max} - \frac{\omega_{\max} - \omega_{\min}}{t_{\max}} \cdot t \tag{12}$$

where $\omega_{\max}$ and $\omega_{\min}$ are the maximum and minimum values of ω, respectively, and $t_{\max}$ is the limit numbers of optimization iteration.

Performing the NF-GMDH and PSO algorithms is a parallel action in each PD. Two fuzzy rules were used to model the neuro-fuzzy in each PD. NF-GMDH-PSO has nine input variables and one output. Throughout modeling the NF-GMDH-PSO model, 15 PDs were produced in the first layer. After that, the second layer was generated using 15 PDs from the first layer. This process could be continued until minimum error of training network is obtained. The NF-GMDH-PSO model with three layers was generated throughout optimization process. Training error of optimization process was 0.00348. The hybridization of the NF-GMDH network and the PSO algorithm within a
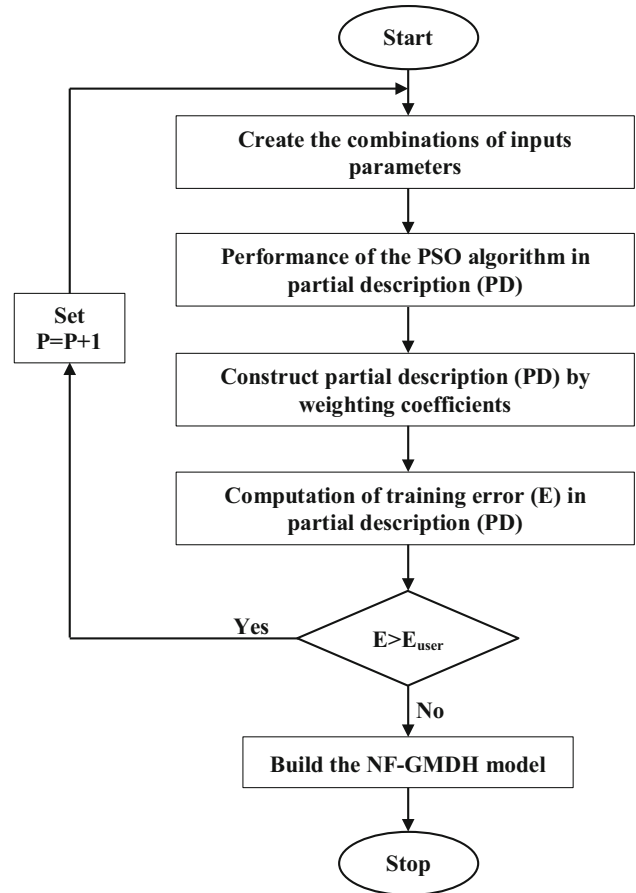

Fig. 3 Flowchart of the NF-GMDH-PSO

parallel process is illustrated in Fig. 3. The value of the control parameters of the PSO algorithm is presented in Table 1. Selections of the control parameters were conducted from experiences of previous researches (e.g., Shi and Eberhart 1998). Two fuzzy rules were applied to develop each PD. Hence, 90 fuzzy rules were used to build three layers of NF-GMDH-PSO network. From performing the training stage, many partial descriptions for the first layer are given as follows:

$$(\text{Log}W)_1^1 = 0.7216 \exp\left[-\frac{(\sigma_0' - 0.4508)^2}{1.4754} - \frac{(D_r - 0.4508)^2}{1.4754} \right]$$
$$+ 0.3289 \exp\left[-\frac{(\sigma_0' - 0.8116)^2}{0.1764} - \frac{(D_r - 0.8116)^2}{0.1764} \right] \tag{13}$$

$$(\text{Log}W)_2^1 = 0.8183 \exp\left[-\frac{(D_r - 0.4291)^2}{1.5} - \frac{(FC - 0.4291)^2}{1.5} \right]$$
$$+ 1.5 \exp\left[-\frac{(D_r - 1.4291)^2}{0.2106} - \frac{(FC - 1.4291)^2}{0.2106} \right] \tag{14}$$

Table 1 Values of the PSO properties for prediction of the strain energy

Parameter	Range
Omega	0.04–0.09
Number of particles	50
Number of variables	6
Maximum iteration	200
Error	0.00001
C_1 and C_2	2.5
Weighting coefficients	0.1–1.5

$$(\text{Log}W)_3^1 = 1.259\exp\left[-\frac{(FC-0.8079)^2}{0.0367} - \frac{(C_u-0.8079)^2}{0.0367}\right]$$
$$+ 0.7822\exp\left[-\frac{(FC-0.2654)^2}{0.8352} - \frac{(C_u-0.2654)^2}{0.8352}\right]$$

(15)

The superscript and subscript of each parameter present the number of pertaining layer and partial description, respectively.

2.3 Model Performance

In order to examine the robustness of the proposed models, the coefficient of determination (R^2), mean absolute percentage error (MAPE) and root-mean-squared error (RMSE) between the measured and predicted strain energy required to induce liquefaction (W) were obtained according to the following equations:

$$R^2 = \frac{\sum_{i=1}^{n}(x_i^m)^2 - \sum_{i=1}^{n}(x_i^m - x_i^p)^2}{\sum_{i=1}^{n}(x_i^m)^2}$$

(16)

$$\text{MAPE} = \frac{1}{n}\sum_{i=1}^{n}\left|\frac{x_i^m - x_i^p}{x_i^m}\right| \times 100$$

(17)

$$\text{RMSE} = \sqrt{\frac{\sum_{i=1}^{n}(x_i^m - x_i^p)^2}{n}}$$

(18)

where n is the number of data and x_i^m and x_i^p are measured and predicted values, respectively.

3 Experimental Database

A wide-ranging database was used from previously published laboratory tests for development of the model (Towhata and Ishihara 1985; Arulmoli et al. 1992; Liang 1995; Green 2001). The database contains cyclic triaxial, cyclic torsional shear and simple shear tests. These experimental studies were conducted on sand and silty sands (Baziar and Jafarian 2007). The database includes 284 element tests data.

The database was divided into two separate groups denoted as training and testing sets consisting of 75 and 25% data, respectively. Once the training of the model has been successfully accomplished, the performance of the trained model is validated using the validation data, which have not been used as the part of model building process (Heidari 2008). The data division process was performed so that the main statistical parameters of the training and testing subsets (i.e., maximum, minimum, mean and standard deviation) become close to each other. For this purpose, a trial selection procedure was carried out and the most possible consistent division was determined (Masters 1993). Descriptive statistics of the data groups variables used in the model development are presented in Table 2.

In the present study, the most important parameters that affect the strain energy required for triggering liquefaction were selected based on the previous studies on the liquefaction potential assessment. The parameters initial mean effective confining pressure, σ'_0 (kPa), relative density after consolidation, D_r (%), mean grain size, D_{50} (mm),

Table 2 Descriptive statistics of the variables used in the models development

Variables		All data				Training set				Testing set			
		Max.[a]	Min.[b]	Mean	SD[c]	Max.	Min.	Mean	SD	Max.	Min.	Mean	SD
Inputs	σ'_0 (kPa)	294	41.1	98.88	27.86	294	41.1	98.33	27.57	294	41.1	100.5	28.85
	Dr (%)	105.1	−44.5	47.60	33.63	105.1	−44.5	48.80	33.31	97.9	−36.5	43.99	34.58
	FC (%)	100	0	20.44	26.32	100	0	22.02	28.47	100	0	15.68	17.76
	D_{50} (mm)	0.46	0.03	0.234	0.13	0.46	0.03	0.23	0.131	0.46	0.03	0.248	0.126
	C_u	5.88	1.57	2.39	1.02	5.88	1.57	2.41	1.023	5.88	1.57	2.31	1.01
	C_c	1.61	0.74	0.952	0.196	1.61	0.74	0.945	0.194	1.61	0.74	0.971	0.201
Output	Log W (J/m³)	4.544	2.477	3.267	0.451	4.544	2.477	3.252	0.44	4.44	2.49	3.313	0.519

[a] Maximun

[b] Minimum

[c] Standard deviation

uniformity coefficient, C_u, coefficient of curvature, C_c, fines content, FC (%), used as input parameters, and measured strain energy density required for occurrence of soil liquefaction, W (J/m^3), was the single output variable. Parameters σ'_0 and D_r represent initial density of soils, and they were referred as intergranular contact density. Also, C_u, C_c and D_{50} are grain size distribution parameters and have been used to capture the grain size characteristic. In addition, FC is individually considered as a factor which controls the potential of pore pressure buildup. It is noteworthy that further experimental and statistical studies are needed to reflect the effect of other effective parameters such as mode of shear and degree of saturation (Saikia and Chetia 2014) on the evaluation of liquefaction potential.

The results of centrifuge tests (Dief 2000) as validation set were also employed in addition to the training and testing sets for further examination and generalization of the model performance.

4 Results

Numerous runs were performed with various initial settings, and the performance of the developed model was analyzed for each run. Consequently, the best model was selected according to statistical criteria such as R^2, MAPE and RMSE. In addition, a comprehensive parametric study was performed to monitor the behavior of each model versus variations of input variables. Proposed NF-GMDH-based model that was selected as most appropriate model was constituted by six input parameters (σ'_0, D_r, FC, D_{50}, C_u and C_c) and one output (Log W).

Precision of the proposed model is examined by plotting the measured versus predicted values of the strain energy density required for occurrence of soil liquefaction, W, for training, testing and all data as shown in Figs. 4 and 5, respectively. The values of R^2, MAPE and RMSE are equal to 0.928, 1.404 and 0.059, respectively, for training set (Fig. 4) and 0.868, 2.197 and 0.118, respectively, for testing set (Fig. 5).

In order to confirm sufficient generalization for future predictions, centrifuge validation tests (Dief 2000) were used as another testing set. Dief (2000) performed these tests on Nevada and Reid Bedford clean sands and LSFD silty sand at Case Western Reserve University. He processed the recorded accelerations and lateral displacements of the laminar box segments using lumped mass models and estimated the shear stress–strain history at different depths in centrifuge models (Baziar and Jafarian 2007). Since these accumulated dissipated energies were calculated up to liquefaction triggering, they represent the capacity of their corresponding soils similar to experimental database. Figure 6 depicts measured versus
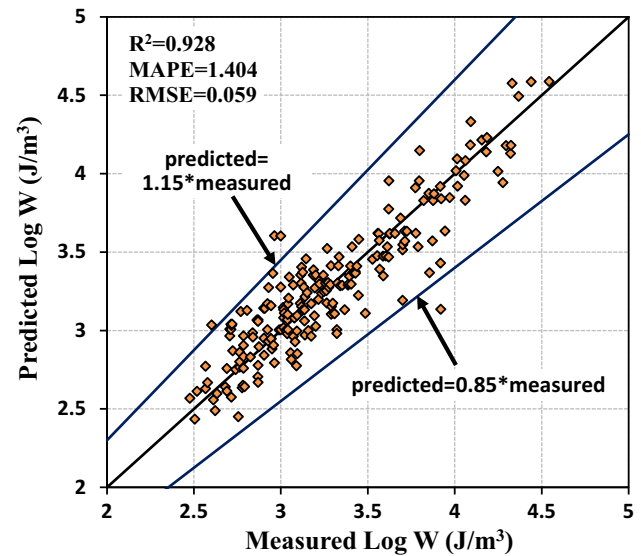

Fig. 4 Measured versus predicted values of strain energy for training dataset
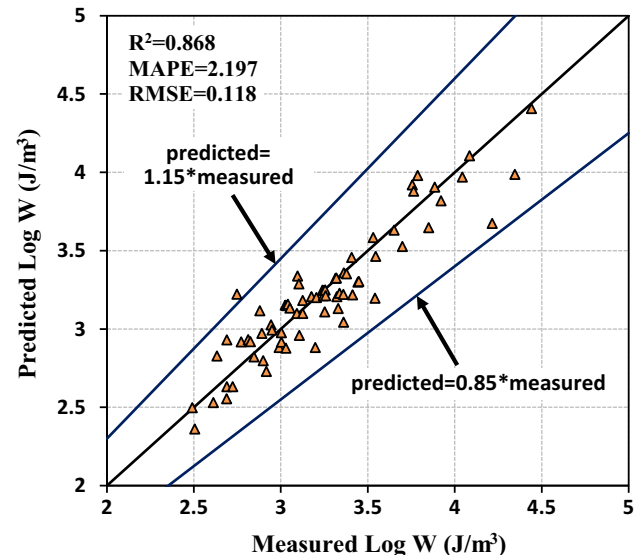

Fig. 5 Measured versus predicted values of strain energy for testing dataset

predicted energy density for the centrifuge validation dataset. The values of R^2, MAPE and RMSE for this dataset were obtained equal to 0.801, 2.101 and 0.101, respectively. In fact, the evolved model has obtained high accuracy for both testing and validation sets.

The results shown in Figs. 4, 5 and 6 indicate reasonable good performance of NF-GMDH-based model for assessment of required strain energy to induce liquefaction because the predicted values are satisfactorily distributed between two lines illustrating 0.85 and 1.15 times of measured values for training and testing datasets and 0.9 and 1.1 times for centrifuge dataset.
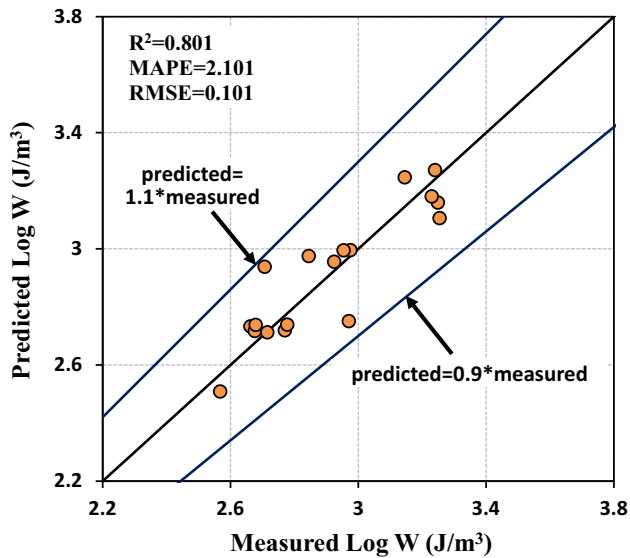
Fig. 6 Measured versus predicted values of strain energy for centrifuge validation set

Table 3 Target statistical parameters of NF-GMDH-based model

Group	Performance		
	R^2	MAPE	RMSE
Training	0.928	1.404	0.059
Testing	0.868	2.197	0.118
All data	0.891	1.896	0.074
Validation (centrifuge tests)	0.801	2.101	0.101

The values of statistical parameters of neuro-fuzzy group method of data handling (NF-GMDH)-based model for training, testing and all datasets are presented in Table 3. R^2, MAPE and RMSE values for centrifuge validation set are also shown in this table.

4.1 Model Accuracy and Sensitivity Analysis

Difference between the measured values of logarithm of strain energy (Log W) to the values predicted by the NF-GMDH-based model as relative error, for both training and testing datasets, is shown in Fig. 7. As the scattering increases in this figure, the accuracy of the model consequently decreases. It is observed that the developed model can predict the strain energy required for occurrence of soil liquefaction with reasonable accuracy because the relative error is satisfactorily distributed between two lines illustrating ± 0.3 J/m^3 relative error.

Figure 8 shows the normalized strain energy (i.e., the ratio of the measured to the predicted Log W values) versus the predicted logarithm of strain energy values. This figure demonstrates that the average value of the normalized
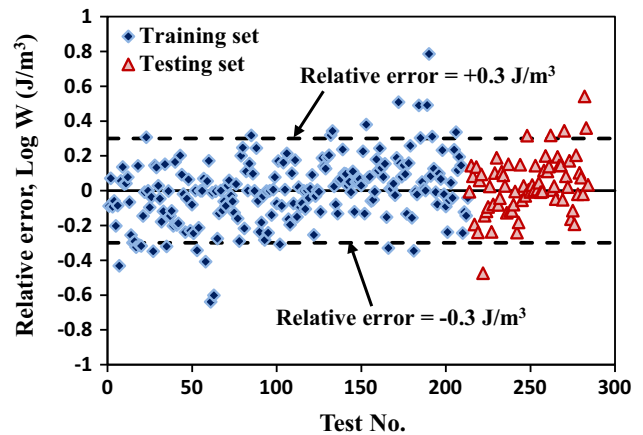

Fig. 7 Relative error between the experimental and NF-GMDH-based predicted values of strain energy
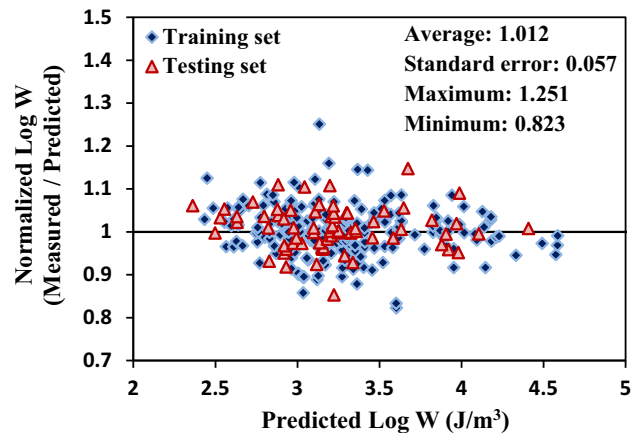

Fig. 8 Normalized strain energy values versus the predicted Log W values

Log W is 1.012 which confirms that the predictions are reasonable. In addition, the maximum and the minimum values of the ratio of the measured to the predicted Log W values were 1.251 and 0.823, respectively.

Further investigation on the model performance under various conditions was conducted through a parametric analysis. This part of the study was performed to evaluate whether the NF-GMDH-based model matches its prediction to those measured in experimental investigations. For this purpose, variations of inputs parameters on the amount of strain energy required to induce liquefaction were studied, while the other parameters were kept constant at their mean values in the database (Table 2).

Variation of strain energy predicted by neuro-fuzzy group method of data handling (NF-GMDH) model against percentage of fines content (FC) at different levels of relative density (D_r) is shown in Fig. 9. This figure includes three curves obtained by the developed NF-GMDH model for the relative densities of 40, 60 and 80%. The predicted
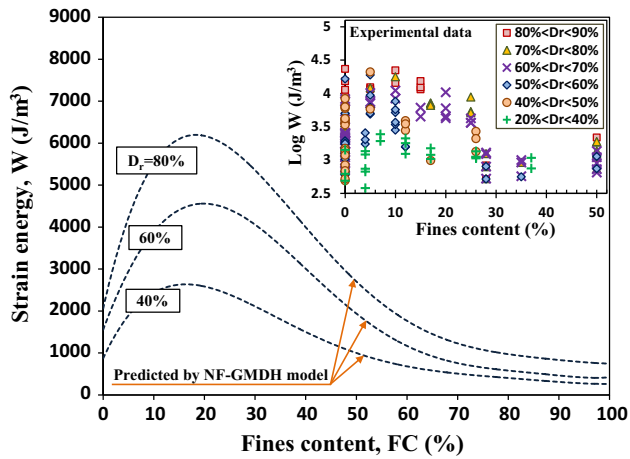
Fig. 9 Variation of W predicted by NF-GMDH-based model versus fines content at different levels of relative density, the experimental data are also superimposed on the plot

Fig. 10 Variation of W predicted by NF-GMDH-based model versus relative density at different levels of mean grain size, the experimental data are also superimposed on the plot

curves were evaluated as a function of FC for $\sigma'_0 = 100$ kPa, $D_{50} = 0.25$ mm, $C_u = 2.4$ and $C_c = 0.95$. Some of the measured data in the range of $20\% < D_r < 90\%$ were also overlaid in Fig. 9 in order to demonstrate how the experimental results of strain energy vary with increasing FC and D_r. As shown in Fig. 9, the amount of strain energy required up to liquefaction triggering initially increases with increment of fines content (FC) up to about 15–20% and then continuously decreases for further increase in FC. Subsequently, the decrement rate of W declines for larger FC. Comparison between the results of the parametric study for FC and D_r (Fig. 9) and experimental database confirms the obtained results and satisfactory performance of the NF-GMDH-based model. The trends observed in Fig. 9 are inconsistent with the findings of some previous studies (Carraro et al. 2003; Hazirbaba and Rathje 2009; Baziar et al. 2011) on the effects of fines content on liquefaction resistance. Also, on the basis of cyclic undrained triaxial tests on Yatesville silty sand, Polito and Martin (2001) reported an increase and then a decrease in liquefaction resistance against increase in percentage of fines content (FC).

Figure 10 depicts variation of strain energy, W, versus relative density, D_r, at different levels of mean grain size, $D_{50} = 0.1, 0.25, 0.4$ mm, while the other parameters were kept constant at their mean values in the dataset (Table 2). The measured data are superimposed on the plot. According to Fig. 10, the amount of W required for liquefaction onset increases with increase in D_r and D_{50}. A similar trend for dependency of W to D_r and D_{50} has been observed in the experimental data.

The effect of relative density on strain energy (W) is more considerable for higher D_{50} values (coarser soil) (Fig. 10). In other words, NF-GMDH-based curves (Fig. 10) show that with increase in mean grains size (D_{50}),
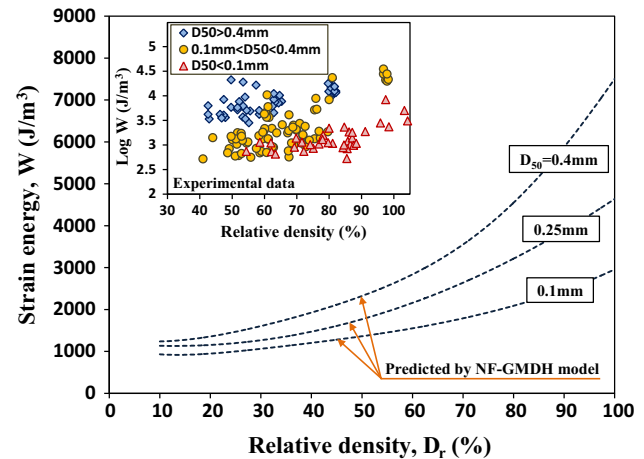
the increment rate of strain energy increases. This finding is in qualitatively good agreement with the results of laboratory studies carried out by Liang (1995). They concluded that the strain energy of coarser soil is higher than that of finer soil. Liang (1995) also reported that the effect of D_r on W is more pronounced for coarse-grained soils in comparison with the fine-grained soils.

4.2 Comparison with the Previous Recommendations

For comparison purpose, predictions of previously recommended relationships (Table 4) are used. There are several studies that have focused on the strain energy-based evaluation of liquefaction potential of soil. On the basis of undrained cyclic tests and centrifuge modeling, various relationships were developed using multiple linear regression (MLR) for strain energy required to induce liquefaction in sands and silty sands (Figueroa et al. 1994; Liang 1995; Dief and Figueroa 2001). Using wide-ranging database of soil element tests, Baziar and Jafarian (2007) developed a MLR-based equation for estimation of W. Alavi and Gandomi (2012) recommended their correlations using genetic programming (GP), linear genetic programming (LGP) and multi-expression programming (MEP). Two different combinations of the influencing variables were considered for the development of their correlations. The first combination of inputs parameters include σ'_0, D_r (i.e., MEP-I and LGP-I models); the other combination consisted of σ'_0, D_r, FC, D_{50} and C_u (i.e., GP, MEP-II and LGP-II models).

The measured results are plotted in Fig. 11a–l against predictions of the developed NF-GMDH model and previous published relationships (Table 4). These comparisons (Fig. 11a–l) confirm that the neuro-fuzzy group method of

Table 4 Relationships for prediction of strain energy required to induce liquefaction of soil

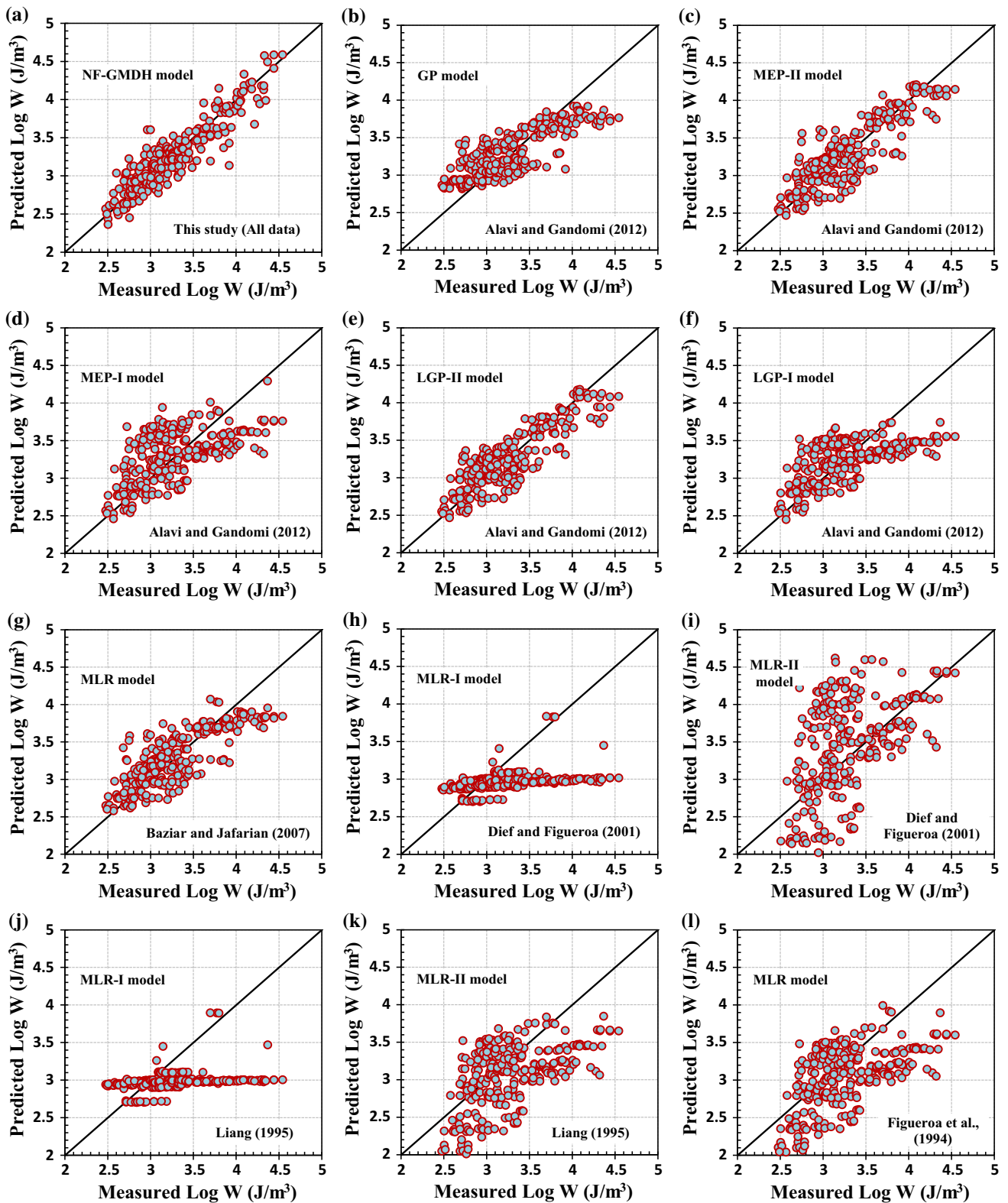| References	Relationship	Model
Figueroa et al. (1994)	$LogW = 2.002 + 0.00477\sigma_0' + 0.0116D_r$	MLR
Liang (1995)	$LogW = 2.062 + 0.0039\sigma_0' + 0.0124D_r$	MLR-I
Liang (1995)	$LogW = 2.484 + 0.00471\sigma_0' + 0.00052D_r$	MLR-II
Dief and Figueroa (2001)	$LogW = 1.164 + 0.0124\sigma_0' + 0.0209D_r$	MLR-I
Dief and Figueroa (2001)	$LogW = 2.4597 + 0.00448\sigma_0' + 0.00115D_r$	MLR-II
Baziar and Jafarian (2007)	$Log\,W = 2.1028 + 0.004566\sigma_0' + 0.005685D_r + 0.001821FC - 0.02868C_u + 2.0214D_{50}$	MLR
Alavi and Gandomi (2012)	$LogW = 2.5 + \left(\dfrac{\sigma_0'}{60} \times \dfrac{D_r+40}{150}\right) - 5 \times \left(\dfrac{\sigma_0'}{300} \times \dfrac{D_r+40}{150}\right)^2$	LGP-I
Alavi and Gandomi (2012)	$LogW = \dfrac{5}{4} \times \left\{\left(\dfrac{\sigma_0'}{150} \times \dfrac{D_r+40}{150} \times \dfrac{D_{50}}{0.5}\right) + \left(\dfrac{D_r+40}{150} \times \dfrac{D_{50}}{0.5}\right) + \left[\left(\dfrac{D_r+40}{150} \times \dfrac{D_{50}^2}{0.25}\right) \times \left(\dfrac{\sigma_0'}{300} + \dfrac{D_{50}}{0.5} - \left(\dfrac{\sigma_0'}{100} - \dfrac{6(FC+40)}{150} + \dfrac{4C_u}{6}\right)^2 - 1\right)\right]\right\} + 2$	LGP-II
Alavi and Gandomi (2012)	$Log\,W = 2.5 + \left(\dfrac{\sigma_0'}{60} \times \dfrac{D_r+40}{150} \times \left(1 - \dfrac{\sigma_0'}{600}\right)\right)$	MEP-I
Alavi and Gandomi (2012)	$LogW = 2.5 + \dfrac{D_r+40}{30} \times \left[\dfrac{\sigma_0'}{600} - D_{50} \times \left(\dfrac{FC+40}{300} + D_{50} \times \left(\dfrac{\sigma_0'}{150} - \dfrac{D_{50}}{0.5} \times \left(\dfrac{\left(\frac{\sigma_0'}{300}\right)^2}{2} + \dfrac{\frac{FC+40}{75}\cdot\frac{C_u}{3}}{\left(\frac{FC+40}{150}\right)} + 1\right) + \dfrac{\left(\frac{\sigma_0'}{300}\right)^2}{4}\right) - 0.5\right)\right]$	MEP-II
Alavi and Gandomi (2012)	$LogW = \left[\dfrac{\left(\left(7 - \left(\frac{\sigma_0'}{300} + \frac{D_r+40}{150} + \frac{D_{50}^2}{0.25}\right)\right) - \left(\frac{\sigma_0'}{300} \times \left(\frac{D_r+40}{150} - \frac{FC+40}{150}\right)\right)\right) + \frac{C_u}{6}}{20}\right]$	GP

Fig. 11 Comparison between the experimental Log *W* versus predicted values from various models: This study (**a**), Alavi and Gandomi (2012) (**b–f**), Baziar and Jafarian (2007) (**g**), Dief and Figueroa (2001) (**h**, **i**), Liang (1995) (**j**, **k**), Figueroa et al. (1994) (**l**)

Table 5 Comparison between performances of the proposed model and the previous models for liquefaction assessment

Model	Performance		
	R^2	MAPE	RMSE
This study (All data), NF-GMDH	0.891	1.896	0.074
Alavi and Gandomi (2012), GP	0.622	6.812	0.277
Alavi and Gandomi (2012), MEP-II	0.718	5.935	0.239
Alavi and Gandomi (2012), MEP-I	0.335	9.148	0.367
Alavi and Gandomi (2012), LGP-II	0.740	5.663	0.229
Alavi and Gandomi (2012), LGP-I	0.355	8.628	0.362
Baziar and Jafarian (2007), MLR	0.645	6.530	0.269
Dief and Figueroa (2001), MLR-I	0.185	15.860	0.638
Dief and Figueroa (2001), MLR-II	0.329	10.760	0.520
Liang (1995), MLR-I	0.129	11.824	0.518
Liang (1995), MLR-II	0.303	10.800	0.471
Figueroa et al. (1994), MLR	0.325	11.539	0.466

data handling (NF-GMDH) model can reasonably predict the strain energy for liquefaction triggering.

Table 5 presents the values of R^2, MAPE and RMSE for the developed NF-GMDH-based model and the Log W values estimated by other statistical equations for liquefaction assessment. Although the MLR-based correlations of Dief and Figueroa (2001), Liang (1995) and Figueroa et al. (1994) yield accurate estimations for their experimental dataset, it is clearly observed in Table 5 that their recommendations were generally unable to accurate prediction of Log W for the current experimental database, which is more comprehensive in comparison with the previous datasets. The results presented in Table 5 confirm higher precision of the proposed model with respect to the previous studies.

5 Summary and Conclusions

In this paper, a relatively large database including laboratory tests including cyclic triaxial, cyclic torsional shear and simple shear tests on sand and silty sands was used. Powerful intelligent tool (i.e., neuro-fuzzy group method of data handling, NF-GMDH) was utilized to develop a model, for prediction of strain energy required for liquefaction onset (W). Also, the particle swarm optimization (PSO) algorithm is applied in topology design of the NF-GMDH model. Based on the experimental observations in the gathered experimental database as well as the previous studies on sandy soils, six parameters: initial mean effective confining pressure (σ'_0), relative density (D_r), fines content (FC), mean grain size (D_{50}), uniformity coefficient (C_u) and coefficient of curvature (C_c), were used as input parameters to develop the NF-GMDH-based model. In

addition, results of several centrifuge tests, which were not used during model development, were employed for further validation of the proposed model. The proposed model showed a reasonably good performance for all element tests ($R^2 = 0.891$, MAPE $= 1.896$, RMSE $= 0.074$) and centrifuge datasets ($R^2 = 0.801$, MAPE $= 2.101$, RMSE $= 0.101$). The relative error of strain energy (W) values of the developed NF-GMDH-based model is approximately below ± 0.3 J/m^3.

A parametric analysis was performed to investigate the behavior of the NF-GMDH model under different conditions and to compare model behavior with those observed in the experimental studies. The results show that the amount of strain energy required up to liquefaction triggering (W) initially increases with increment of fines content (FC) up to about 15–20% and then continuously decreases with increase in percentage of fines. Also, W increases with increase in relative density and mean grains size (D_{50}). These variation trends of the developed model are in good agreement with the previously published experimental results. Comparisons between the performances of the developed NF-GMDH-based model and previously recommended relationships (Table 4) for liquefaction assessment have been done. It is clearly observed that the model of neuro-fuzzy group method of data handling (NF-GMDH) yields a much better performance than the previous recommendations (Fig. 11; Table 5). Therefore, the results of comparison confirm high precision of the developed model for estimation of strain energy required to trigger liquefaction in sandy soils.

Although the influence of most effective parameters on liquefaction potential was captured in the proposed GMDH-based model of strain energy, some parameters (e.g., mode of shear) were ignored. It is clear that a detailed study on this subject can potentially result in a more rigorous energy-based model. Moreover, the methodology presented in this paper is introduced as a method that is currently under development and will need the use of larger databases before it can be proposed for general application to the current practice of liquefaction design. Definitely, more studies on the energy-based approach are needed to develop robust and generalized models for estimating soil liquefaction potential.

References

Alavi AH, Gandomi AH (2012) Energy-based numerical models for assessment of soil liquefaction. Geosci Front 3(4):541–555

Arulmoli K, Muraleetharan KK, Hosain MM, Fruth L S (1992) VELACS laboratory testing program. Soil data report, the earth technology corporation, Irvine, Calif. Report to the National Science Foundation, Washington, DC

Baykasoglu A, Cevik A, Ozbakir L, Kulluk S (2009) Generating prediction rules for liquefaction through data mining. Expert Syst Appl 36:12491–12499

Baziar MH, Jafarian Y (2007) Assessment of liquefaction triggering using strain energy concept and ANN model: capacity energy. Soil Dyn Earthq Eng 27(12):1056–1072

Baziar MH, Jafarian Y, Shahnazari H, Movahed V, Tutunchian MA (2011) Prediction of strain energy-based liquefaction resistance of sand–silt mixtures: an evolutionary approach. Comput Geosci 37(11):1883–1893

Carraro JAH, Bandini P, Salgado R (2003) Liquefaction resistance of clean and nonplastic silty sands based on cone penetration resistance. J Geotech Geoenviron Eng 129(11):965–976

Dabiri R, Askari F, Shafiee A, Jafari MK (2011) Shear wave velocity-based liquefaction resistance of sand-silt mixtures: deterministic versus probabilistic approach. Iran J Sci Technol Trans B Eng 35:199–215

Dief HM, Figueroa JL (2001) Liquefaction assessment by the energy method through centrifuge modeling. In: Zeng XW (ed) Proceedings of the NSF international workshop on earthquake simulation in geotechnical engineering. CWRU, Cleveland

Dief H M (2000) Evaluating the liquefaction potential of soils by the energy method in the centrifuge. Ph.D dissertation, Department of Civil Engineering, Case Western Reserve University, Cleveland, OH

Dobry R, Ladd RS, Yokel FY, Chung RM, Powell D (1982) Prediction of pore water pressure build-up and liquefaction of sands during earthquakes by the cyclic strain method. National Bureau of Standards, US Department of Commerce, US Governmental Printing Office, Building Science Series, Washington, DC

Figueroa JL, Saada AS, Liang L, Dahisaria MN (1994) Evaluation of soil liquefaction by energy principles. J Geotech Geoenviron Eng 20(9):1554–1569

Green RA (2001) Energy-based evaluation and remediation of liquefiable soils. Ph.D dissertation, Virginia Polytechnic Institute and State University, Blacksburg, VA

Hazirbaba K, Rathje EM (2009) Pore pressure generation of silty sands due to induced cyclic shear strains. J Geotech Geoenviron Eng 135(12):1892–1905

Heidari A (2008) Artificial neural network (theory and application with MATLAB). Nazeran, Esfahan (In Persian)

Heidari A (2010) Optimum design of structures for earthquake induced loading by genetic algorithm using wavelet transform. Adv Appl Math Mech 2(1):107–117

Heidari A (2011) Calculation of frequency of retaining wall by back propagation neural network. Asian J Civil Eng 12(3):267–278

Heidari A, Salajegheh E (2006) Time history analysis of structures for earthquake loading by wavelet networks. Asian J Struct Eng 7:155–168

Hwang HS (2006) Fuzzy GMDH-type neural network model and its application to forecasting of mobile communication. Comput Ind Eng 50:450–457

Ishihara K, Yasuda S (1975) Sand liquefaction in hollow cylinder torsion under irregular excitation. Soils Found 15(1):45–59

Ivakhnenko AG (1971) Polynomial theory of complex systems. IEEE Trans Syst Man Cybern 1:364–378

Jafarian Y, Sadeghi Abdollahi A, Vakili R, Baziar MH, Noorzad A (2011) On the efficiency and predictability of strain energy for the evaluation of liquefaction potential: a numerical study. Comput Geotech 38(6):800–808

Jafarian Y, Haddad A, Javdanian H (2014) Predictive model for normalized shear modulus of cohesive soils. Acta Geodyn Geomater 11(1):89–100

Javdanian H, Haddad A, Mehrzad B (2012) Experimental and numerical investigation of the bearing capacity of adjacent footings on reinforced soil. Electron J Geotech Eng 17(R):2597–2617

Javdanian H, Jafarian Y, Haddad A (2015) Predicting damping ratio of fine-grained soils using soft computing methodology. Arab J Geosci 8(6):3959–3969

Kalantary F, Ardalan H, Nariman-Zadeh N (2009) An investigation on the Su-NSPT correlation using GMDH type neural networks and genetic algorithms. Eng Geol 104:144–155

Kennedy J, Eberhart RC (1995) Particle swarm optimization. In: Proc. of the fourth IEEE int. conf. on neural networks, pp 1942–1948

Lee KL, Fitton JA (1969) Factors affecting the cyclic loading strength of soil. Vib Eff Earthq Soils Found 450:71–95

Liang L (1995) Development of an energy method for evaluating the liquefaction potential of a soil deposit. Ph.D dissertation, Department of Civil Engineering, Case Western Reserve University, Cleveland, OH

Madala HR, Ivakhnenko AG (1994) Inductive learning algorithms for complex systems modeling. CRC Press, Boca Raton

Masters T (1993) Practical neural network recipes in C++. Academic press, San Diego

McCombie P, Wilkinson P (2002) The use of the simple genetic algorithm in finding the critical factor of safety in slope stability analysis. Comput Geotech 29:699–714

Nagasaka K, Ichihashi H, Leonard R (1995) Neuro-fuzzy GMDH and its application to modeling grinding characteristics. Int J Prod Res 33(5):1229–1240

Najafzadeh M (2014) Neuro-fuzzy GMDH system based particle swarm optimization for prediction of scour depth at downstream of grade control structures. Eng Sci Technol Int J 18(1):42–45

Najafzadeh M, Azamathulla HM (2013a) Group method of data handling to predict scour depth around bridge piers. Neural Comput Appl 23:2107–2112

Najafzadeh M, Azamathulla HM (2013b) Neuro-fuzzy GMDH systems to predict the scour pile groups due to waves. J Comput Civil Eng. doi:10.1061/(ASCE)CP.1943-5487.0000376

Najafzadeh M, Lim SY (2014) Application of improved neuro-fuzzy GMDH to predict scour downstream of sluice gates. Earth Sci Inform 8(1):187–196

Najafzadeh M, Barani GA, Azamathulla HM (2013a) GMDH to prediction of scour depth around vertical piers in cohesive soils. Appl Ocean Res 40:35–41

Najafzadeh M, Barani GA, Hessami Kermani MR (2013b) GMDH network based back propagation algorithm to predict abutment scour in cohesive soils. Ocean Eng 59:100–106

Najafzadeh M, Barani GA, Azamathulla HM (2014a) Prediction of pipeline scour depth in clear-water and live-bed conditions using group method of data handling. Neural Comput Appl 24:629–635

Najafzadeh M, Barani GA, Hessami-Kermani MR (2014b) Group method of data handling to predict scour at downstream of a ski-jump bucket spillway. Earth Sci Inform 7(4):231–248

National Research Council (1985) Liquefaction of soils during earthquakes. National research council report CETS-EE-001. National Academy Press, Washington

NCEER (1997) In: Proceedings of the NCEER workshop on evaluation of liquefaction resistance of soils. National Center for Earthquake Engineering Research, Technical Report No. NCEER970022, State University of New York at Buffalo, New York

Oh HJ, Pradhan B (2011) Application of a neuro-fuzzy model to landslide-susceptibility mapping for shallow landslides in a tropical hilly area. Comput Geosci 7(9):1264–1276

Ohtani T, Ichihashi H, Miyoshi T, Nagasaka K (1998) Orthogonal and successive projection methods for the learning of neurofuzzy GMDH. Inform Sci 110(1):5–24

Onwubolu GC (2008) Design of hybrid differential evolution and group method in data handling networks for modeling and prediction. Inform Sci 178:3618–3634

Penumadu D, Zhao R (1999) Triaxial compression behavior of sand and gravel using artificial neural networks (ANN). Comput Geotech 24:207–230

Polito CP, Martin JR (2001) Effects of nonplastic fines on the liquefaction resistance of sands. J Geotech Geoenviron Eng 127(5):408–415

Rakhshandehroo GR, Ghadampour Z (2011) A combination of fractal analysis and artificial neural network to forecast groundwater depth. Iran J Sci Technol Trans B Eng 35:121–130

Saikia R, Chetia M (2014) Critical review on the parameters influencing liquefaction of soils. Int J innov Res Sci Eng Technol 3:110–116

Salajegheh E, Heidari A (2004) Optimum design of structures against earthquake by adaptive genetic algorithm using wavelet networks. Struct Multidiscip Optim 28:277–285

Seed HB, Idriss IM (1971) Simplified procedure for evaluating soil liquefaction potential. J Soil Mech Found Div 97:1249–1273

Seed HB, Mori K, Chan CK (1975) Influence of seismic history on the liquefaction characteristics of sands. Report EERC 75-25, Earthquake Engineering Research Center, University of California, Berkeley

Shahin MA, Maier HR, Jaksa MB (2002) Predicting settlement of shallow foundations using neural networks. J Geotech Geoenviron Eng 128(9):785–793

Shi Y, Eberhart R C (1998) A modified swarm optimizer, In: Proc. of the IEEE int. conf. on evolutionary computation, Anchorage, pp 69–73

Tabesh M, Dini M (2009) Fuzzy and neuro-fuzzy models for short-term water demand forecasting in Tehran. Iran J Sci Technol Trans B Eng 33:61–77

Towhata I, Ishihara K (1985) Shear work and pore water pressure in undrained shear. Soils Found 25(3):73–84

Whitman RV (1971) Resistance of soil to liquefaction and settlement. Soils Found 11(4):59–68

Youd T, Idriss I, Andrus R, Arango I, Castro G, Christian J, Dobry R, Finn W, Harder LJ, Hynes M, Ishihara K, Koester J, Liao S, Marcuson W, Martin G, Mitchell J, Moriwaki Y, Power M, Robertson P, Seed R, Stokoe K II (2001) Liquefaction resistance of soils: summary report from the 1996 NCEER and 1998 NCEER/NSF workshops on evaluation of liquefaction resistance of soils. J Geotech Geoenviron Eng 127(10):817–833